

# A Smart Control Circuit with Breakdown and Charging Completion Detection to Implement Power-off Function for Lithium-iron Phosphate Battery Charger

Jye-Chau Su,<sup>1</sup> Cheng-Tao Tsai,<sup>2\*</sup> and Tsair-Chun Liang<sup>3</sup>

<sup>1</sup>Department of Electronic Engineering, National Chin-Yi University of Technology, Taichung 41170, Taiwan

<sup>2</sup>Department of Electrical Engineering, National Chin-Yi University of Technology, Taichung 41170, Taiwan

<sup>3</sup>Department of Electronic Engineering, National Kaohsiung University of Science and Technology, Kaohsiung 824005, Taiwan

(Received December 30, 2021; accepted March 29, 2022)

**Keywords:** lithium-iron phosphate battery, LED

In this paper, a smart control circuit with breakdown and charging completion detection to implement a power-off function for a lithium-iron phosphate battery charger is proposed. The smart control circuit of the lithium-iron phosphate battery charger has a simple structure and its advantages are as follows. (1) When the lithium-iron phosphate battery is fully charged during charging, the control circuit can implement the power-off function of the lithium-iron phosphate battery charger. Therefore, it can effectively increase the life of the lithium-iron phosphate battery. (2) In the event of a short circuit or under a low voltage condition, the control circuit can rapidly turn off the power source of the lithium-iron phosphate battery. (3) By incorporating a simple sensing circuit, the fault conditions in the lithium-iron phosphate battery during charging can be easily detected. Therefore, it can effectively decrease the probability of electrical accidents. Additionally, the charging status of the lithium-iron phosphate battery is shown by LED indicators, which allow users to easily determine fault conditions. Finally, a 51.7 V<sub>dc</sub> and 150 W prototype of the lithium-iron phosphate battery charger is built and implemented. Experimental results are presented to verify the performance and feasibility of the smart control circuit with breakdown and charging completion detection to implement the power-off function for the lithium-iron phosphate battery charger.

## 1. Introduction

Large amounts of fossil fuels are used, and thus global carbon monoxide emissions have increased significantly, leading to rapid global warming. According to data records, more than 24% of global carbon monoxide and particulate matter emissions come from fuel-powered vehicles.<sup>(1,2)</sup> In Taiwan, fuel-powered motorcycles are generally popular. Because these motorcycles are suitable for riding in the streets and alleys of cities, people are not delayed by traffic jams. To reduce the carbon monoxide and particulate matter emissions by fuel powered motorcycles, which cause serious air pollution, the government provides a subsidy to people who

---

\*Corresponding author: e-mail: [cttsai@ncut.edu.tw](mailto:cttsai@ncut.edu.tw)  
<https://doi.org/10.18494/SAM3816>

buy electric motorcycles or electric bicycles for personal transportation. These vehicles have the advantages of nonpolluting, high energy efficiency, and low noise. They are a type of convenient transportation in urban areas and can effectively solve the problem of air pollution.<sup>(3–5)</sup>

The electric motorcycles or electric bicycles require a high-performance battery. The high-performance lithium-iron phosphate battery used as the power sources of these vehicles is widely accepted because of its many advantages. (1) It belongs to the category of green energy and does not cause air pollution. (2) Charging and discharging temperatures do not easily rise. (3) It can provide a high discharging power (large current can be generated instantly) and long cycle lives. However, the price of the lithium-iron phosphate battery determines its quality. The inside of a low-quality lithium-iron phosphate battery has many impurities, which induce the crystallization of the negative electrode. This phenomenon causes internal short circuits of the lithium-iron phosphate battery during charging, which can cause explosion and other serious electrical accidents.<sup>(6–8)</sup> Therefore, when breakdown conditions are detected during the charging of the lithium-iron phosphate battery via an AC-to-DC charger, the charging power of the lithium-iron phosphate battery must be effectively and quickly shut down. The chargers of the lithium-iron phosphate battery mainly use AC-to-DC isolated high-efficiency switching power converters for electric vehicles or electric bicycles.<sup>(9–11)</sup> The advantages of these converters are the safety of electrical isolation and high conversion efficiency.<sup>(12,13)</sup> However, their main disadvantage is that they cannot detect breakdown or charging completion to implement the power-off function for the lithium-iron phosphate battery.<sup>(14–16)</sup> Therefore, electrical accidents frequently happen.

To overcome the above problems, a smart control circuit with breakdown and charging completion interconnecting an AC-to-DC charger is proposed, as shown in Fig. 1. The AC-to-DC

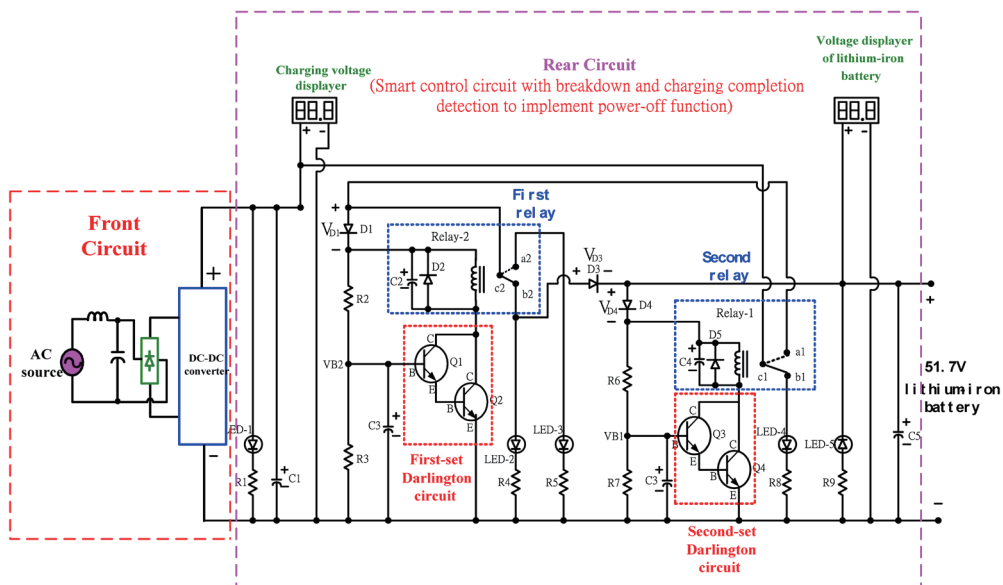


Fig. 1. (Color online) A smart control circuit with breakdown and charging completion interconnects with the AC-to-DC charger to implement power-off function.

charger consists of two circuits. The front circuit is an AC-to-DC isolated high-efficiency switching power converter and the rear circuit is a smart control circuit. The proposed smart control circuit has a simple structure, which has the following advantages. When the lithium-iron phosphate battery is fully charged or induces breakdown (short circuit and low voltage) during charging processes, the control circuit can rapidly implement the power-off function of the AC-to-DC charger. Therefore, it can effectively increase the life of the lithium-iron phosphate battery and decrease the probability of electrical accidents.

## 2. Structure Analysis of Smart Control Circuit

Figure 1 shows that the proposed smart control circuit with breakdown and charging completion detection to implement the power-off function has a simple structure. It consists of Darlington circuits, power relays, and LED displays. To effectively drive the power relay, a simple and low-cost Darlington circuit is selected, as shown in Fig. 2. The Darlington circuit consists of two transistors with a type number of 2N5551 to drive a 48 V<sub>dc</sub> power relay. The following equations are used to calculate the base current ( $I_B$ ) and collecting current ( $I_C$ ) of the transistors.

$$I_B = \frac{(V_{th} - V_{BE1} - V_{BE2})}{R_{th}} \quad (1)$$

$$I_C = \beta^2 I_B \quad (2)$$

Here,  $V_{th} = (\frac{R_2}{R_1 + R_2})V_A$ ,  $R_{th} = (\frac{R_1 R_2}{R_1 + R_2})$ , and  $\beta$  is the current gain of transistors.

To correctly design and select the values of the resistors ( $R_1$  and  $R_2$ ), an accurate  $I_C$  of the

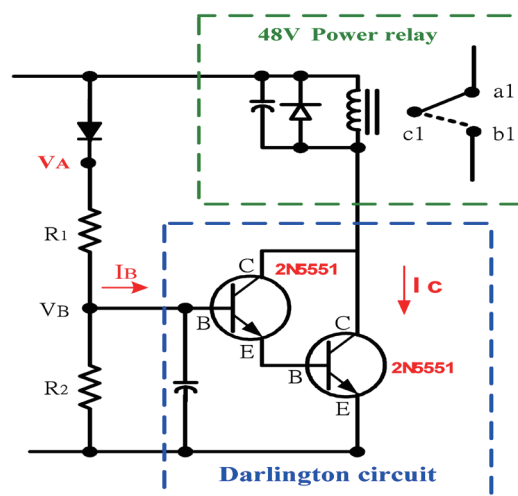


Fig. 2. (Color online) Structure of a Darlington circuit to drive a power relay.

transistor can be obtained from the Darlington circuit. Therefore, the power relay can be easily turned on.

### 3. Operational Principles of Smart Control Circuit

The operational principles of the smart control circuit are divided into four major operating modes. The equivalent circuit of each operating mode is shown in Fig. 3. The following is a brief description of the operating modes of the smart control circuit.

#### Mode 1: The voltage polarity of the lithium-iron phosphate battery and the charging power source is inversely connected.

When the lithium-iron phosphate battery is connected to the charging power source, the control circuit will detect the voltage polarity correctness of the lithium-iron phosphate battery and the charging power source. If the voltage polarity of the lithium-iron phosphate battery and the charging power source is reversely connected, the currents ( $I_C$ ) of the first-set Darlington circuit (Darlington-1) are equal to zero. Therefore, the first-set power relay (Relay-1) is turned off and the indicator LED-5 is turned on. In this operating mode, the lithium-iron phosphate battery cannot charge, causing the reverse connection of the voltage polarity. The equivalent circuit is shown in Fig. 3(a).

#### Mode 2: The internal cells of the lithium-iron phosphate battery have a short current.

When the internal cells of the lithium-iron phosphate battery have a short current, a zero voltage ( $V_{battery} = 0$ ) of the lithium-iron phosphate battery is detected via the smart control circuit. The currents ( $I_C$ ) of the first-set Darlington circuit (Darlington-1) are equal to zero, resulting in the first-set power relay (Relay-1) being turned off and the indicator LED-4 being

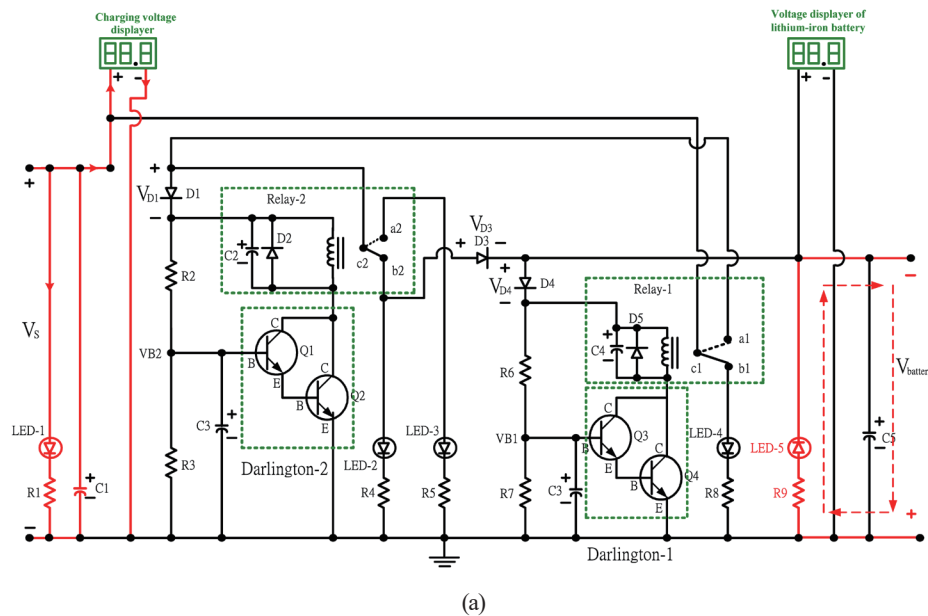
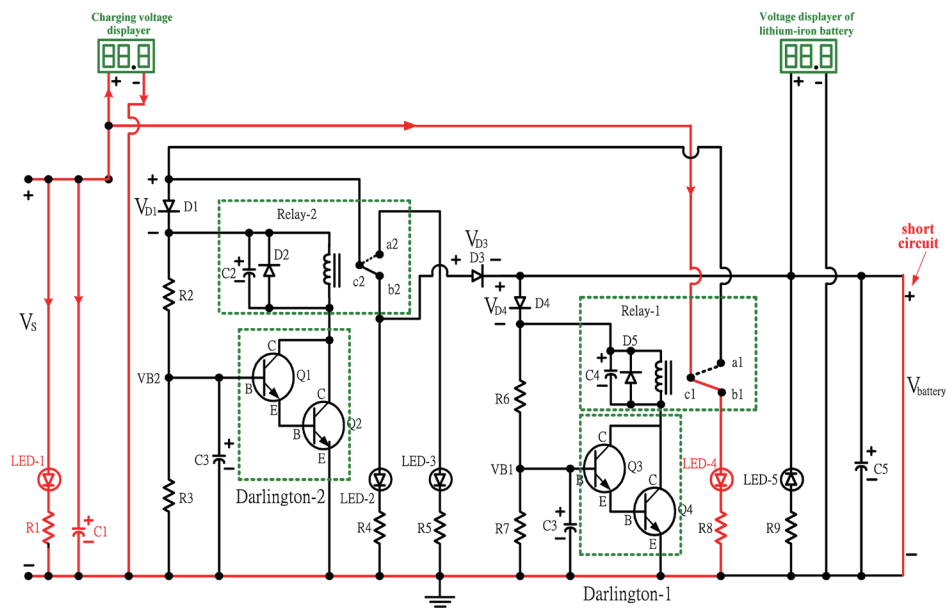


Fig. 3. (Color online) Equivalent circuits of smart control circuit with breakdown and charging completion detection to implement power-off function. (a) Mode 1.

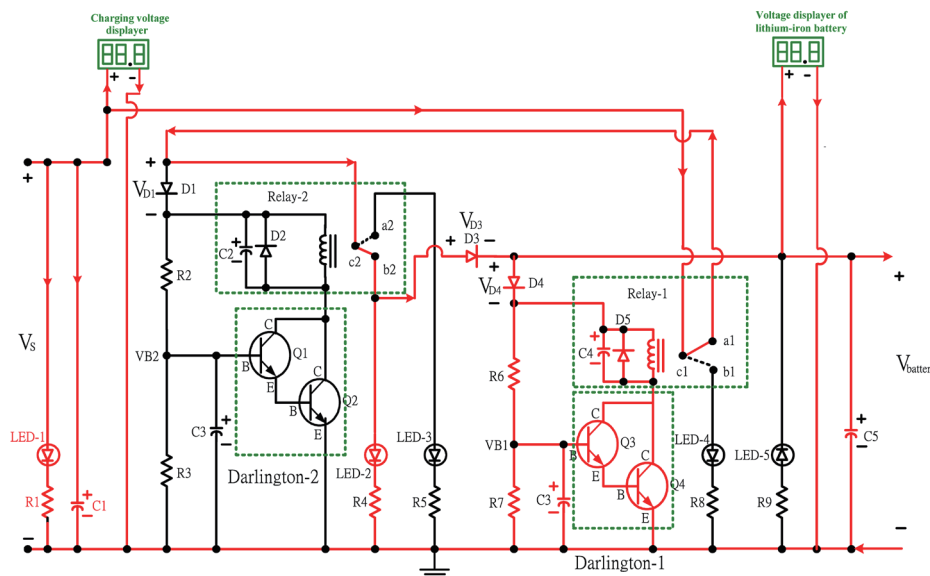
turned on. During this interval, when the internal cells of the lithium-iron phosphate battery have a short current, the charging power source can be turned off immediately. Therefore, it can protect the lithium-iron phosphate battery and avoid electrical accidents. The equivalent circuit is shown in Fig. 3(b).

**Mode 3: The lithium-iron phosphate battery is operated in the charging processes.**

If the lithium-iron phosphate battery does not have reversely connected or short circuits, the currents ( $I_C$ ) of the first-set Darlington circuit (Darlington-1) are other than zero, resulting in the



(b)



(c)

Fig. 3. (Continued) (b) Mode 2. (c) Mode 3.

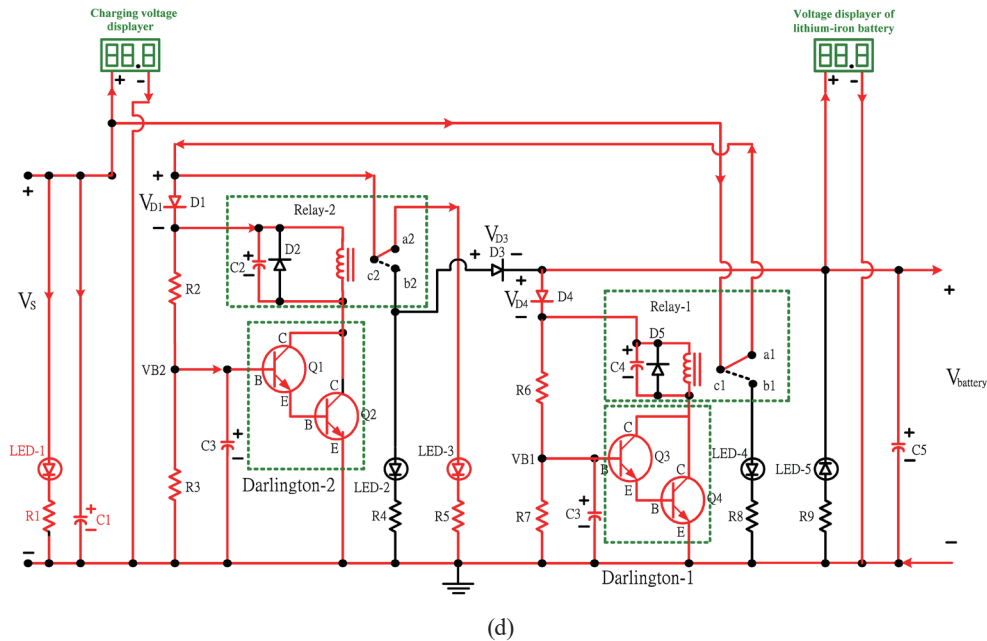


Fig. 3. (Continued) (d) Mode 4.

first-set power relay (Relay-1) being turned on and the indicator LED-2 also being turned on. During this interval, the lithium-iron phosphate battery enters a normal charging process. The equivalent circuit is shown in Fig. 3(c).

#### Mode 4: The charging of the lithium-iron phosphate battery is completed.

When the lithium-iron phosphate battery is completely charged, the currents ( $I_C$ ) of the second-set Darlington circuit (Darlington-2) are other than zero, resulting in the second-set power relay (Relay-2) being turned on, the indicator LED-3 also being turned on, and the indicator LED-2 being turned off. During this interval, the charging power source is turned off and overcharging, which decreases the life of the lithium-iron phosphate battery, is avoided. The equivalent circuit is shown in Fig. 3(d).

## 4. Experimental Results

To verify the feasibility of the proposed smart control circuit with breakdown and charging completion detection to implement the power-off function, a 150 W prototype of the AC-to-DC charger interconnecting a smart control circuit is built, as shown in Fig. 1. The specifications of the AC-to-DC charger with a smart control circuit are as follows:

- input voltage:  $V_{in} = 90\text{--}265\text{ V}_{ac}$ ,
- output voltage:  $V_{out} = 51.7\text{ V}_{dc}$ ,
- output current:  $I_o = 2.85\text{ A}$ ,
- output power:  $P_{out} = 150\text{ W}$ .

Figure 4 shows the measured voltage waveforms of the voltage reversely connected to the lithium-iron phosphate battery and the charging power source. It can be seen that the voltage is reversely connected to the lithium-iron phosphate battery, the charging power source is turned

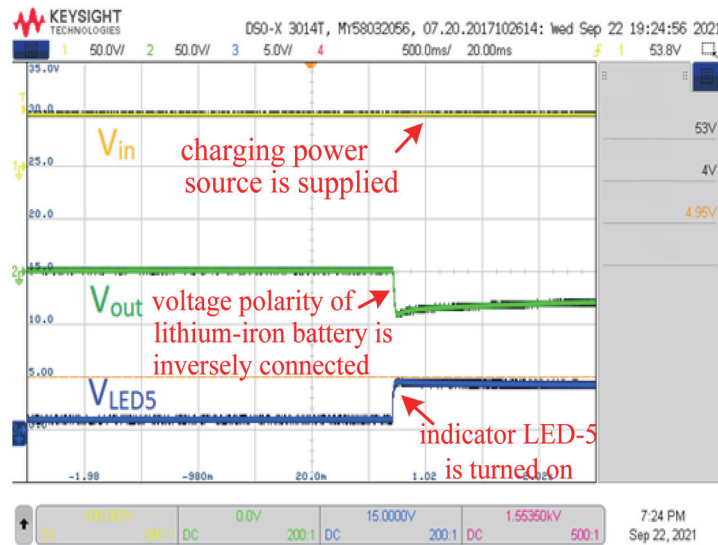


Fig. 4. (Color online) Measured waveforms of voltage reversely connected to the lithium-iron phosphate battery and charging power source.

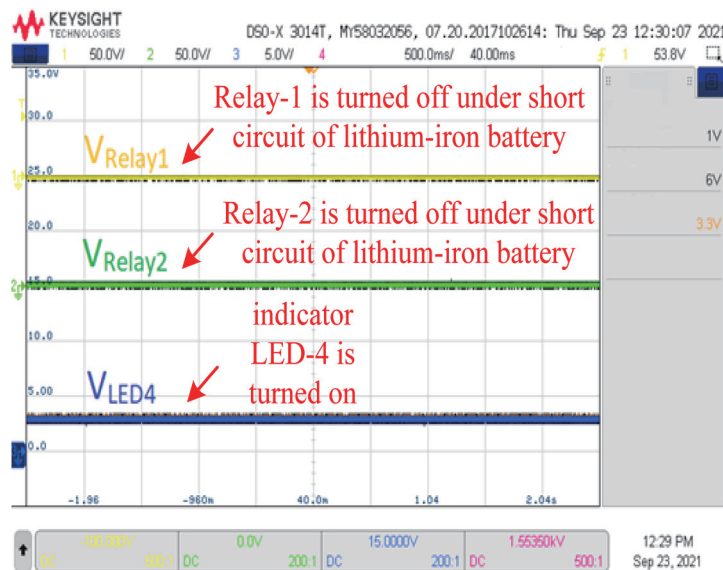


Fig. 5. (Color online) Measured voltage waveforms of Relay-1 and Relay-2 under short circuit of lithium-iron phosphate battery.

off, and the indicator LED-5 is turned on. Figure 5 shows the measured voltage waveforms of Relay-1 and Relay-2 when the internal cells of the lithium-iron phosphate battery have short circuits. It can be seen that Relay-1 and Relay-2 are turned off and the indicator LED-4 is turned on under short-circuit conditions. Figure 6 shows the measured voltage waveforms of Relay-1 and Relay-2 during the charging process of the lithium-iron phosphate battery. It can be seen that Relay-1 is turned on, Relay-2 is turned off, and the indicator LED-2 is turned on. Figure 7 shows

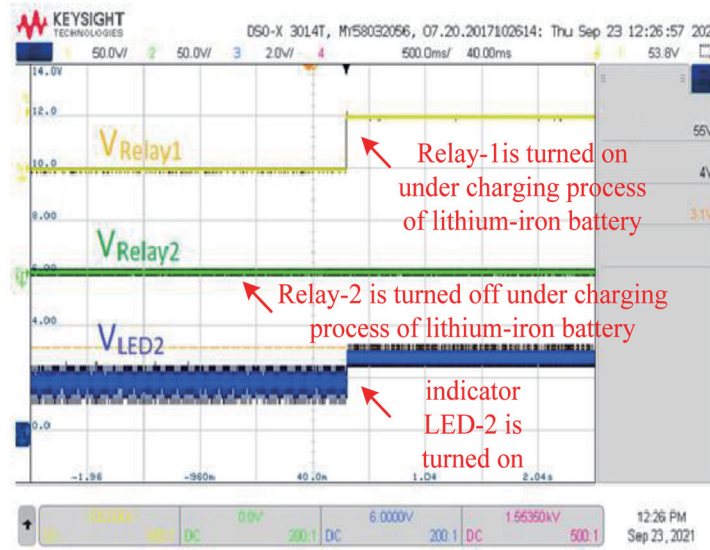


Fig. 6. (Color online) Measured voltage waveforms of Relay-1 and Relay-2 under charging process of lithium-iron phosphate battery.

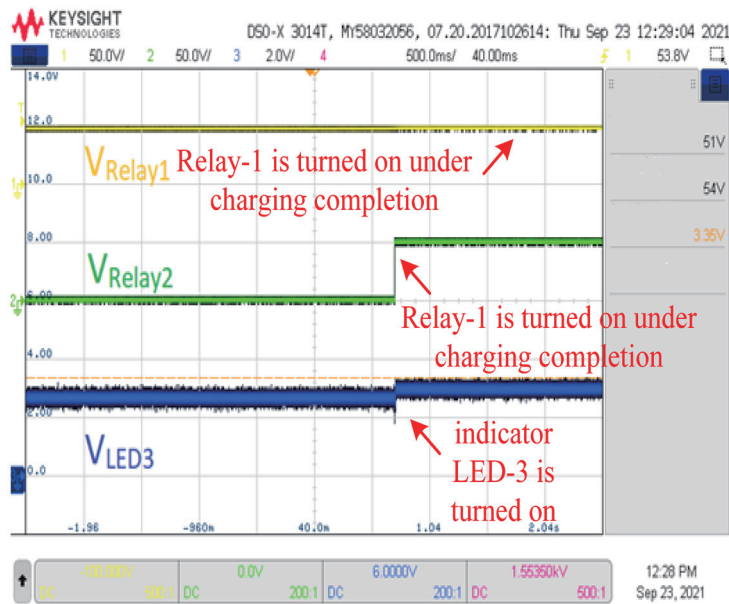


Fig. 7. (Color online) Measured voltage waveforms of lithium-iron phosphate battery at charging completion.

the measured voltage waveforms of Relay-1 and Relay-2 during the charging completion of the lithium-iron phosphate battery. It can be seen that Relay-1 and Relay-2 are turned on and the indicator LED-3 is also turned on. Figure 8 shows the proposed smart control circuit with breakout and charging completion detection to implement power-off function for the lithium-iron phosphate battery charger.



Fig. 8. (Color online) Proposed smart control circuit with breakout and charging completion detection to implement power-off function for lithium-iron phosphate battery charger.

## 5. Conclusions

In this paper, a proposed smart control circuit with breakout and charging completion detection to implement the power-off function for lithium-iron chargers has been built and implemented. It uses a simple structure to implement the power-off function when the breakout and charging completion of the lithium-iron phosphate battery have occurred. Therefore, it can effectively increase the life of the lithium-iron phosphate battery and decrease the probability of electrical accidents. Experimental results have confirmed that the proposed smart control circuit with breakout and charging completion detection to the implement power-off function is suitable for the lithium-iron phosphate battery charger.

## Acknowledgments

This work was supported by National Chin-Yi University of Technology, Taiwan

## Author Contributions

All authors contributed to this paper. Cheng-Tao Tsai wrote the paper, Jye-Chau Su contributed to the design and obtained the experimental results of the proposed circuits, and Tsair-Chun Liang proofread the paper.

## Conflicts of Interests

The authors declare that there are no conflicts of interest regarding the publication of this paper.

## References

- 1 S. R. Bull: Proc. The IEEE **89** (2001) 1216. <https://doi.org/10.1109/5.940290>
- 2 K. Kobayashi, H. Matsuo, and Y. Sekine: IEEE Trans. Ind. Electron. **53** (2006) 281. <https://doi.org/10.1109/TIE.2005.862250>
- 3 A. A. Tropina, L. Lenarduzzi, S. V. Marasov, and A. P. Kuzmenko: IEEE Trans. Plasma Sci. **37** (2009) 2286. <https://doi.org/10.1109/TPS.2009.2029692>
- 4 Y. Nishi, K. Katayama, J. Shigetomi, and H. Horie: Proc. 13th Annu. Battery Applications and Advances Conf. (IEEE, 1998) 31. <https://doi.org/10.1109/BCAA.1998.653834>
- 5 B. T. Kuhn, G. E. Pitel, and P. T. Krein: Proc. Vehicle Power and Propulsion Conf. (IEEE, 2005) 55. <https://doi.org/10.1109/VPPC.2005.1554532>
- 6 J. Zhang, D. D.-C. Lu, and T. Sun: IEEE Trans. Ind. Electron. **57** (2010) 1041. <https://doi.org/10.1109/TIE.2009.2028336>
- 7 R. J. Wai, C. Y. Lin, R. Y. Duan, and Y. R. Chang: IEEE Trans. Power Electron. **54** (2007) 354. <https://doi.org/10.1109/TIE.2006.888794>
- 8 S. M. Chen, T. J. Liang, L. S. Yang, and J. F. Chen: IEEE Trans. Power Electron. **26** (2011) 1146. <https://doi.org/10.1109/TPEL.2010.2090362>
- 9 T. Mishima and M. Nakaoka: IEEE Trans. Power Electron. **26** (2011) 3896. <https://doi.org/10.1109/TPEL.2011.2132146>
- 10 C. A. Gallo, F. L. Tofoli, and J. A. C. Pinto: IEEE Trans. Power Electron. **25** (2010) 775. <https://doi.org/10.1109/TPEL.2009.2033063>
- 11 M. Uno and A. Kukita: IEEE Trans. Power Electron. **30** (2015) 3077. <https://doi.org/10.1109/TPEL.2014.2331312>
- 12 H. Wang, H. S.-H. Chung, and A. Ioinovici: IEEE Trans. Power Electron. **27** (2012) 2242. <https://doi.org/10.1109/TPEL.2011.2173588>
- 13 Y. Park, B. Jung, and S. Choi: IEEE Trans. Power Electron. **27** (2012) 3568. <https://doi.org/10.1109/TPEL.2012.2187342>
- 14 T. J. Liang and J. H. Lee: IEEE Trans. Ind. Electron. **62** (2015) 4492. <https://doi.org/10.1109/TIE.2014.2386284>
- 15 S. W. Lee and H. L. Do: IEEE Trans. Power Electron. **32** (2017) 1375. <https://doi.org/10.1109/TPEL.2016.2549029>
- 16 C. T. Tsai and C. L. Shen: IEEJ Trans. Elect. Electron. Eng. **8** (2013) 182. <https://doi.org/10.1002/tee.21838>